Title	Wheeltracking Fatigue Simulation of Bituminous Mixtures
Authors(s)	Hatman, Anton M.; Gilchrist, M. D.; Nolan, D. B.
Publication date	2001-06-15
Publication information	Road Materials and Pavement Design, 2 (2): 141-160
Publisher	Informa UK (Taylor & Francis)
Item record/more information	http://hdl.handle.net/10197/5964
Publisher's statement	This is an electronic version of an article published in Road Materials and Pavement Design (2001) 2(2): 141-160. Road Materials and Pavement Design is available online at: www.tandfonline.com, DOI: http://dx.doi/org/10.3166/rmpd.2.141-160.
Publisher's version (DOI)	10.3166/rmpd.2.141-160

Wheeltracking fatigue simulation of bituminous mixtures

A.M. Hartman — M.D. Gilchrist (✉) — D. Nolan

Mechanical Engineering Department

National University of Ireland, Dublin

Belfield

Dublin 4

IRELAND

Michael.Gilchrist@ucd.ie

ABSTRACT: *In order to better simulate the dynamic effects of a rolling wheel travelling over an asphalt pavement, and to better understand the initiation and growth of cracks in bituminous pavement layers, a wheeltracking fatigue simulation facility was developed. This experimental facility permitted the testing of large slab specimens (305x305x50mm) using dynamic wheel loadings. The slab specimens were supported on a soft elastomeric foundation that simulated overlay behaviour on top of a weak pavement structure. Digital photography and image analysis techniques were utilised to monitor the initiation and propagation of fatigue cracks on the bottom of these slabs. Two standard Irish mixtures, a Dense Base Course Macadam (DBC) and Hot Rolled Asphalt (HRA), were evaluated with the fatigue simulation facility. Crack damage was seen to initiate on the bottom face of the slab specimen in a direction parallel to the direction of wheel travel. These cracks would interconnect to form a full width crack that propagated through the depth of the slab. Under similar loading conditions the DBC mix had significant lower fatigue strength (two orders of magnitude).*

KEY WORDS: *bituminous mixture, fatigue, crack growth, wheeltracking*

1. Introduction

Fatigue testing of bituminous road building materials tends to focus on characterising the fatigue behaviour of relatively small specimens in the laboratory using mainly uniaxial loading conditions [GIL 97, HAR 00]. The effect of a rolling wheel is very difficult to imitate in these experiments and boundary conditions lead to a pattern of crack initiation and propagation that can be quite different to what is observed in-situ. While these simplified laboratory tests provide information on the relative fatigue behaviour of different mixtures, the success with which this information can be related to behaviour under in-situ tri-axial loading conditions remains questionable [HAR 01a, HAR 01b, OWE 01].

Although laboratory scaled wheeltracking equipment has been used extensively to simulate the development of permanent deformation, its application in fatigue studies has been limited. Commercially available permanent deformation wheeltrackers include the Cooper Research Technology Wheeltracker and the LCPC wheeltracking machine. With these devices, slab specimens are supported on solid foundations that prevent slab flexure and promote failure through densification and shear flow of the tested material.

On a larger scale, numerous accelerated loading test facilities exist throughout the world [TAB 89, GIL 97]. These facilities test full-scale pavements and allow the interaction between different forms of pavement distress to be studied. They do, however, involve enormous initial investment and high annual operational and maintenance costs.

In 1975 Van Dijk [VAN 75] pioneered the laboratory scale fatigue wheeltracking experiment by performing a series of wheeltracks to validate beam fatigue test results on a wheeltracker developed at the Shell Amsterdam laboratories. Since then wheeltracking work has been reported from Texas [LEE 93], Nottingham [ROW 96], and elsewhere [HAR 99, SAI 00]. Fatigue simulating rolling wheel test configurations that have been developed include (i) those based on reversing wheels, where a wheel traverses back and forth across a section of pavement, (ii) continuous wheels which travel in the same direction at a constant velocity along a section of pavement and (iii) revolving wheels which travel at a constant velocity along a circular section of pavement.

2. Design and construction of facility

While developing the design specifications for a fatigue simulation wheeltracking facility, the basic concepts of the test were evaluated with a prototype tracker. The experimental arrangement, shown in Figure 1, consisted of a wheelfixture that was mounted in a standard shaping machine. The reciprocating action of the shaping machine pushed the wheel over a slab specimen that was housed in a clamping box fixed to the load table of the machine.

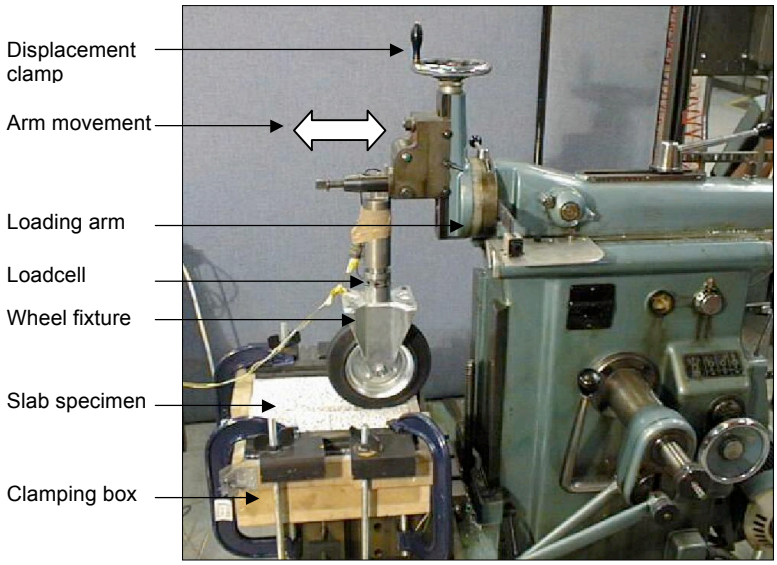

Figure 1. *Development of design specifications for fatigue simulator using a prototype tracker based on the reciprocating action of a shaping machine.*

From these initial tests the following conclusions were drawn:

- In order to induce fatigue cracks that are similar to what is observed in-situ, the slab specimen must be clamped onto solid side supports, as shown in Figure 2 (c). A slab that is only supported by an elastomeric cushion (Figure 2 (a)) results in excessive deformation, slab movement during tracking and very localised cracking. Clamping the slab directly onto a

cushion (Figure 2 (b)) induces forces that counteract the load of the rolling wheel.

- Monitoring cracks on the bottom of slab specimens is very labour intensive. Consequently, it was considered necessary that the design of the facility should permit easy dismantling of the slab so that the underside, from where damage initiates, could be inspected and photographed at intervals.
- A reciprocating wheel action complicates any subsequent interpretation of results. This type of loading doubles the number of wheelpasses over the centre of the specimen; this occurs at higher loading speeds than over any other section of specimen and the direction of loading is not uniform. Over the short distance (305mm) available on the particular standard slab specimen, a segment of the wheel is in constant contact with the slab: this causes both the wheel and slab to heat up and ultimately leads to excessive permanent deformation.
- The shaping machine was operated using displacement control: this resulted in rapid load drop-off and reduced crack growth. In order to perform fatigue tests within a reasonable time span a load controlled loading mode should be used. This is probably most easily achieved through a dead weight system.

With due consideration for the aforementioned design features, an experimental facility that included four pavement monitoring stations was designed around a circular wheel tracking arrangement. The essence of the design involved the use of an existing circular motor driven table which spun two preloaded wheel fixtures around a track, which was fitted with four sample stations as shown in Figure 3.

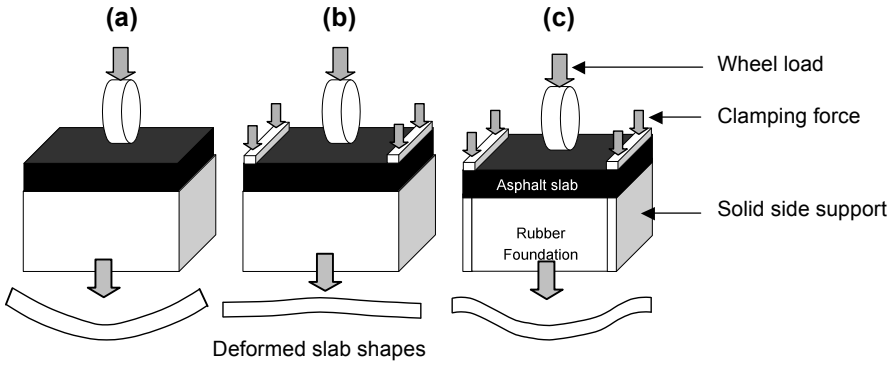

Figure 2. *Schematic illustration of three different slab clamping mechanisms investigated with associated deformed shapes: (a) slab lying freely on rubber foundation; (b) slab clamped down directly on rubber foundation; (c) slab clamped on sides parallel to wheel travel.*

This particular construction ensures that the simulated direction of travel across each pavement specimen is always identical and that the simulated traffic density and velocity, and the weight of axle loadings can also be maintained constant during testing. The substrata conditions under each pavement specimen are made from an elastomeric cushion that can be modified easily by using appropriate materials having different stiffness characteristics.

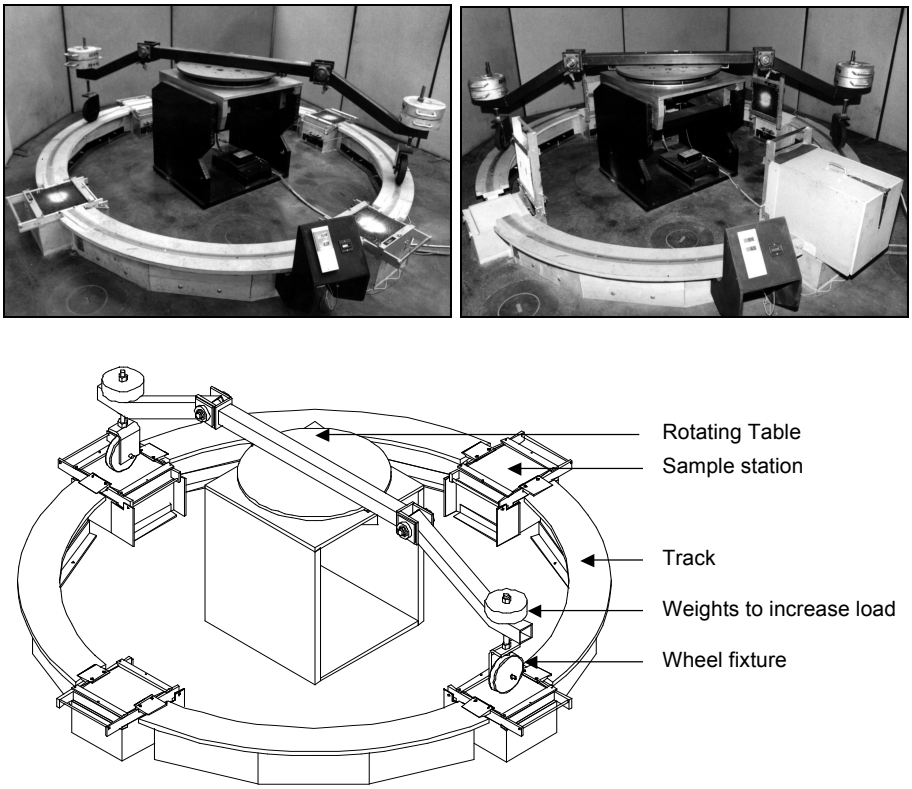

Figure 3. *General layout of rotating fatigue testing facility. Four sample stations house pavement specimens on elastic foundations. (Top left) View of facility during tracking. (Top right) View of facility during crack monitoring with slab specimens turned on their sides and camera box inserted above one slab station.*

The facility was designed to operate on a dead load system with the rotating arms linked through hinged joints to the wheel fixtures. This ensures that the load automatically follows the deformation of the sample, ensuring a load control mode of loading.

The large arc of the track, 3 m diameter, reduces the effect of cornering on the specimen while the influence of centrifugal forces are minimised by the relatively slow operating speed (approximately 3 km/h or 7 rpm). The large track diameter results in near linear travel over the slab and crack failure patterns that are parallel to the clamped specimen sides. Due to the long track length (9.4m) the wheel is in contact with a given slab for only approximately 13% of the time. This, together with the better heat dissipation characteristics of the wooden track, significantly reduced the influence of heating on permanent deformation.

Miniature wheels, 200 mm in diameter with solid rubber tyres, were fitted to the fixtures on the ends of the rotating arms. The width of the wheelpath is 36 mm. The size of the contact area can be varied by changing the dead weight fixed to each wheel fixture and was measured using static tyre imprints. Table 1 summarises the contact areas and tyre pressures associated with the three different loads that were used during testing.

Load (kg)	**Contact area (mm^2)**	**Tyre surface contact pressure (kPa)**
55	1010	545
80	1150	695
100	1290	775

Table 1. *Summary of contact area and tyre pressure for the three load settings.*

Four sample stations, each of which housed a pavement specimen, were incorporated into the track, in order to facilitate the simultaneous testing of multiple samples. An additional four sample stations, giving a total of eight, could be incorporated easily into this design, to double the number of specimens tested in a given period. However, the present study is only concerned with the arrangement of four specimens. Each specimen is clamped in an aluminium frame along its edges, parallel to the tracking direction. This allows the specimen to deform under the influence of the dynamic load. The constraining clamps are fixed to the foundation box, which contains an elastomeric foundation 170mm deep with an elastic stiffness of 2 MPa. This represents a very weak foundation support but it does permit the

pavement specimen to bend under the wheel load without deforming under the influence of gravity.

In order to facilitate and simplify the capturing of images of pavement damage on the bottom face of the slab, the aluminium frame holding the specimen was designed with a hinged joint as shown in Figure 4. By releasing two lock clips, the frame flips back to the vertical position in one single movement, thus revealing the underside of the slab. This allows the insertion of a camera box, housing a digital camera and light source to monitor and record any visible damage.

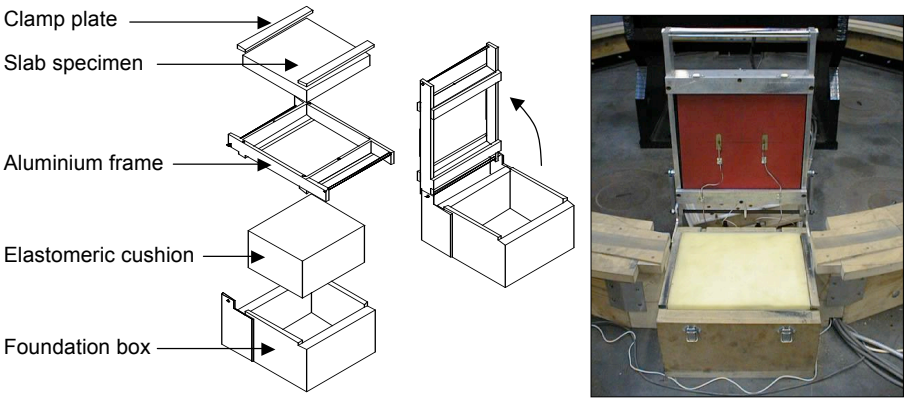

Figure 4. *Layout of a sample station. The foundation box houses the elastic foundation material while the slab specimen is clamped in the aluminium frame. The hinge joining the components allows the specimen to be turned onto its side so that the bottom face can be inspected with ease.*

In order to guide the wheel onto the slab the track was precisely aligned with the top face of the specimen. As the structural integrity of the slab deteriorates, a slight permanent deflection develops across the slab. The main purpose of the present tests was not to isolate fatigue from the effects of creep, but rather was to simulate the initiation and development of fatigue damage within an actual pavement, which would naturally be subjected to both fatigue and creep. The permanent slab deflection across the wheel path was monitored at the centre of the slab during the tests. Most specimens were found to be severely cracked or to have failed catastrophically by the time a significant deformation was reached.

3. Visual monitoring of slab cracking

A procedure using digital image photography was used to monitor the crack development on the bottom face of the slab specimens in the present investigation.

3.1. *Image capturing*

Prior to tracking, the undersides of slab specimens were painted with a quick drying road marking spray-paint. Any cracks or damage were therefore anticipated to show up as black against a white background. A number of thin paint layers were applied until a completely white surface was obtained. A 100x100mm square area was marked directly underneath the wheelpath in the centre of each slab. All crack monitoring was concentrated on this area while all strain monitoring devices were situated away from it.

Fatigue damage that initiates on the underside of the pavement samples inside the square area was monitored using two image capturing methods namely, digital photography and hand traced images that were subsequently digitised. At discrete intervals throughout a test, tracking was stopped and the specimens were turned on their sides. A specially constructed camera housing was then inserted over the sample stations to provide identical photographic distance and lighting conditions during image capture. Digital photographs of the underside of the samples were captured with an Olympus C-840L digital camera. Clear transparent sheets were then placed over the monitoring areas and all visible crack defects marked by hand. The transparencies were subsequently digitised with an optical scanner and reused to monitor cumulative damage. A schematic illustration of the image capture arrangement is shown in Figure 5.

3.2. *Image processing*

The manually traced cracks were scanned as a greyscale image. Selection of the monitoring box (100x100mm square are = 600x600 pixels), clearing of the background and storing of the image data in a compressed format (.JPG) were done using the Ulead PhotoImpact image processing package [ULE 96].

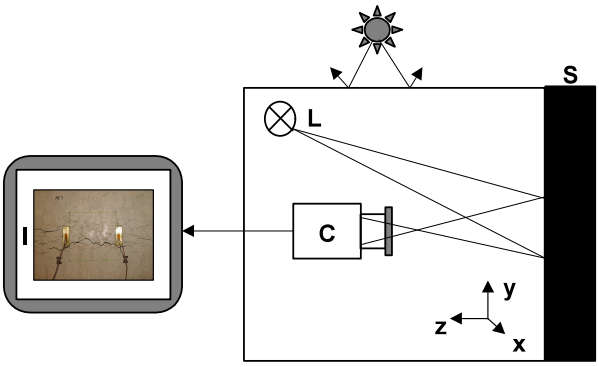

Figure 5. *Schematic of arrangement for digital photography: S = sample; C = camera with frame grabber; L = light source; I = image processing.*

The digital photographs were all in full colour and were 640x480 pixels in size. They also included the area of the slab around the monitoring square area as shown in Figure 6. The monitoring area was 230x230 pixels in size and this was converted to greyscale. The greyscale images were imported into UTHSCSA Image Tool [UTH 96] for image processing and analysis. The dimensions of the monitoring area (100x100mm) were calibrated against the pixel size so that direct dimensional measurements could be established for the digital images. The grey scale images were converted into a binary format (consisting of only pure white and pure black pixels) by applying a threshold value. The selection of this threshold value was achieved by applying a range of thresholds and manually selecting the particular value that best represented the crack damage. This same threshold was then applied to all subsequent images.

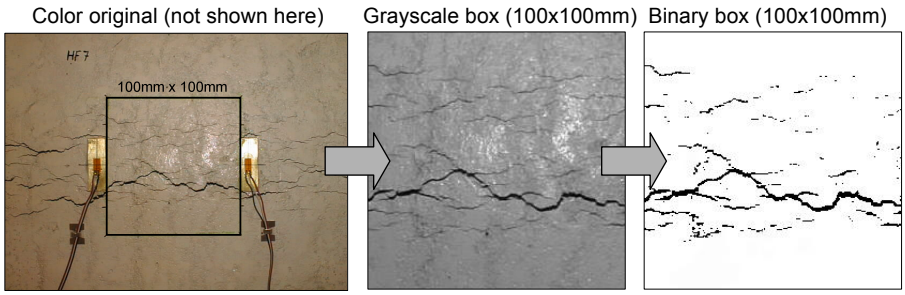

Figure 6. *Manipulation of the original image to select the monitoring area, convert the image to greyscale and apply a threshold to obtain a binary image for crack analysis.*

3.3. *Image analysis*

To calculate the total area of cracks, an algorithm that counts the number of black pixels was applied to the images that were captured with the digital camera. The spatial calibration of this data allowed the area to be given in mm^2. With regard to the images obtained from the manually traced transparencies, no distinction was made between narrow and wide cracks and all visible defects were recorded with a marker of standard width. Using the same analysis routine to calculate the amount of black pixels, but normalising the area against the width of the tracing marker, the actual total crack length was determined.

Measurements of crack direction were also made on the final traced crack network pattern. An image analysis subroutine was used to identify cracks as objects. The major axis angle, i.e., the angle of the longest line drawn through the object to the horizontal, was determined for each object. The major axis angle, normalised to the length of each crack, represents the effective crack direction of each crack.

4. Strain monitoring

The key parameter that is used in asphalt overlay design is the horizontal tensile strain, the critical value of which is at the bottom of the asphalt layer [ULL 87]. Methods for measuring strain are based on various mechanical, optical, acoustic, pneumatic and electric phenomena. One of the most common methods of measuring strain in engineering applications is the use of wire or foil strain gauges. For pavement applications strain gauges are generally selected on the basis of their gauge length, which is based on the maximum aggregate size of the mixture.

To monitor the horizontal tensile strain in the slab specimens, 120ohm foil strain gauges with a gauge length of 10mm were used. To eliminate the influence of aggregates the gauges were glued to thin (0.3mm) brass sheets (12.5x40mm). Brass has a stiffness similar to bituminous mixtures (±2000MPa) and the brass strips were expected to deform in unison with the slab material. Figure 7 shows the basic location of the gauges on a slab. Two gauges were fixed to each slab, one on either side of the crack monitoring square normal to the centre line that runs parallel to the tracking direction. Consequently the gauges measured strains transverse to the tracking direction.

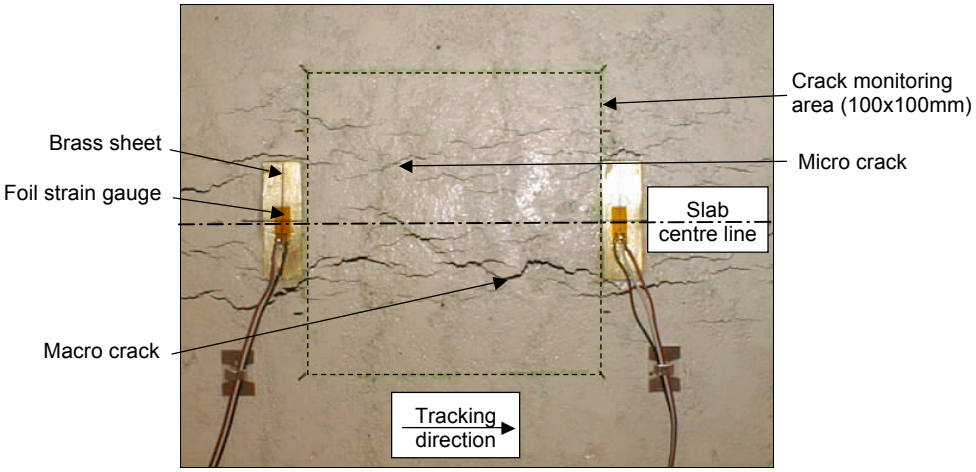

Figure 7. *Strain gauges were positioned on either side of the crack monitoring area, along the centre line of the slab and in a direction perpendicular to wheel travel.*

Strain levels in the slabs can be changed either by adjusting the load, the specimen thickness or the foundation stiffness. During tracking, both the dynamic strain and the total strain were monitored. The dynamic strain is the per cycle strain amplitude of a sample whereas the total strain present within a sample includes strain associated with permanent deformation, as illustrated in Figure 8.

A typical strain pulse as sensed by the two gauges when the wheel moves over a specimen is presented in Figure 9. Gauge 1 is positioned on the wheel entry side of the slab and accordingly reaches a peak value before Gauge 2. The wheel remains in contact with the slab for approximately 0.4s. As the wheel moves off the slab, a permanent level of strain remains in the slab and this dissipates in accordance with the viscoelastic characteristics of the bituminous mixture.

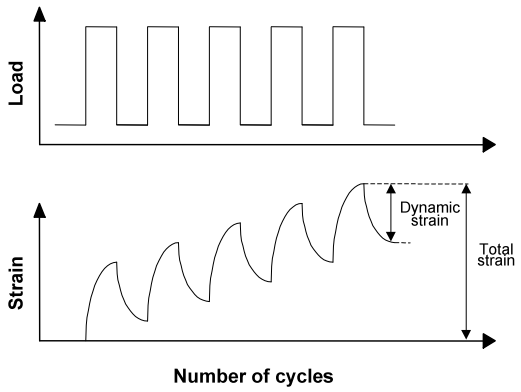

Figure 8. *Typical development of dynamic and total strain during a fatigue test. The viscoelastic response of the bituminous pavement during a given cycle is apparent, together with the gradual increase in strain over numerous load cycles (i.e., permanent deformation).*

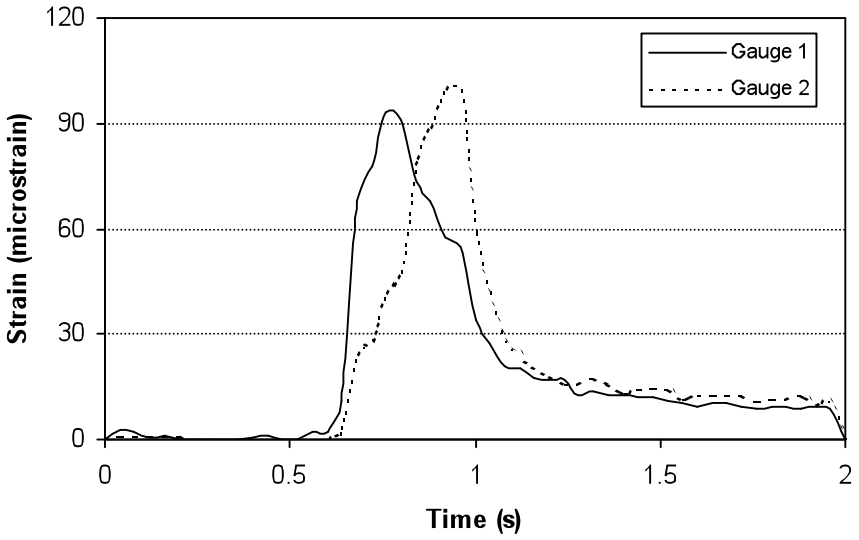

Figure 9. *Typical recorded levels of strain as the loaded wheel moves over a slab specimen.*

5. Experimental test programme

The composition of the two mixtures used in the present investigation is summarised in Table 2. They represent two different grading profiles, namely, an open graded sandy mix (HRA, [BS 92]) and a continuous grading (DBC, [BS 93]), as shown in Figure 10. For both of the mixtures binder contents towards the lower end of the design spectrum were purposely chosen to obtain fatigue prone mixtures. Slab specimens (305Lx305Wx50D) were compacted with a laboratory roller compactor and cured for 24 hour at 60°C after compaction.

Data that was monitored continuously during testing include measurements from strain gauges that were fixed to the bottom of the specimens, digital images of the cracked underside of the slab specimens, the manually traced crack patterns, the permanent slab deflection, and the total number of cycles to failure.

DBC - % by weight passing sieve						
20mm	**14mm**	**10mm**	**6.3mm**	**3.35mm**	**300µm**	**75µm**
98	82	66	52	40	16	4.5
Bitumen content : 4.2% (100 Pen) Target void content : 6% (by volume)						

HRA - % by weight passing sieve					
20mm	**14mm**	**10mm**	**2.36mm**	**212µm**	**75µm**
100	97	80	66	30	10
Bitumen content : 7.3% (50 Pen) Target void content : 4% (by volume)					

Table 2. *Mix constituents.*

Initially, the fatigue simulation experiments were carried out on one set of each of the investigated mixtures. The 100kg load setting, which corresponded to a tyre contact pressure of approximately 775 kPa, was used. The HRA slabs had a fatigue life in excess of 200 000 load cycles and this was achieved after two full weeks of testing. The DBC slabs, tested at the same load level, failed after only 2000 load cycles. Since the fatigue simulation facility was situated within a large laboratory which did not have adequate temperature control, all subsequent tests focused on the DBC mixture as these could be tested within a relatively short time span and thus

reduce the effect of overnight temperature changes. Two extra sets of DBC slabs were accordingly prepared and tested at load levels shown in Table 3. Table 3 also identifies the recorded minimum and maximum slab temperatures during the tests. The HRA samples were tested at lower temperature conditions. Also, the 80kg DBC specimens were tested at a slightly higher temperature. The lack of temperature control is a limitation of the present experimental set-up, which complicates minimising the effects of creep. Modifications to the set-up, which would include environmental temperature control are planned for future experiments.

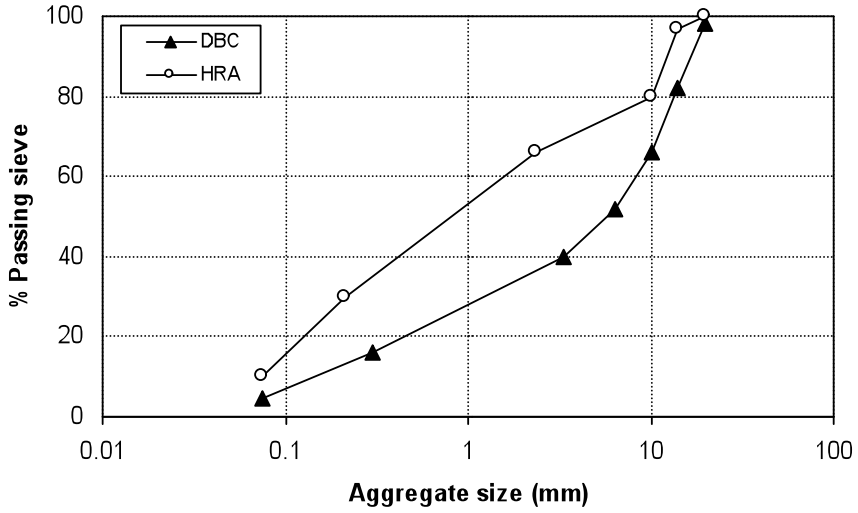

Figure 10. *Aggregate grading of bituminous mixtures under investigation.*

Material	Load (kg)	Contact pressure (kPa)	Temperature (°C)	
			Minimum	Maximum
HRA	100	775	12.6	18.6
DBC	100	775	20.7	23.4
	80	695	23.6	25.3
	55	545	20.5	23.1

Table 3. *Summary of load settings and the specimen temperature range for fatigue simulation tests.*

6. Results and discussion

6.1. *Crack measurements*

Figure 11 summarises the measurement of crack area while measurements of cumulative crack lengths are shown in Figure 12. The general manner in which cumulative crack length varied with fatigue cycles was to initially increase sharply and then increase much more gradually. The rapid initial increase of crack length typically represented 30% of the fatigue life of a specimen. On the other hand, the crack area increased gradually as the test began and progressed and accelerated growth rates were observed close to specimen failure. In general, a larger area of cracking was observed on the DBC specimens. DBC slabs tested at the same load setting also had longer cumulative crack lengths. The total length of cracks measured in the DBC specimens also decreased with reduced test loads.

Rather than one main crack appearing under the wheel track, what was observed was that small individual cracks opened along the bottom of a sample, these interconnected and combined to establish a crack network. Once a full width crack had formed, this crack propagated through the depth of the slab. Two stages can thus be distinguished: a crack initiation stage, during which the network of cracks is formed and a crack propagation stage, during which the cracks propagate through the depth of the slab and thus only appear to grow wider on the slab surface. The reduced rate of increase of cumulative crack length can thus be explained as crack propagation, during which the cracks increase in width and depth rather than any new cracks being formed.

The orientation of the final crack pattern to the direction of wheel loading was determined and this is summarised in Table 4. Figure 13 shows typical examples of the final crack pattern within both the HRA and DBC mixtures. Cracks tended to remain relatively parallel to the direction of wheel travel. Since the slabs were clamped on the sides that were perpendicular to the direction of wheel travel, this allowed slab bending and consequently cracking occurred primarily in that direction. As the test load decreased, the direction of cracking deviated slightly from the horizontal. The HRA and DBC slabs that were tested at the same loading conditions displayed similar crack orientations.

Material	Contact pressure (kPa)	Effective crack direction, C_D^{eff} (°)				
		Slab 1	Slab 2	Slab 3	Slab 4	Average
HRA	775	15.3	14.6	15.5	18.7	16.0
DBC	775	14.2	16.4	17.0	19.9	16.9
	695	23.3	25.2	31.5	19.0	24.8
	545	40.2	37.0	21.6	25.8	31.2

Table 4. *Summary of effective crack direction measurements.*

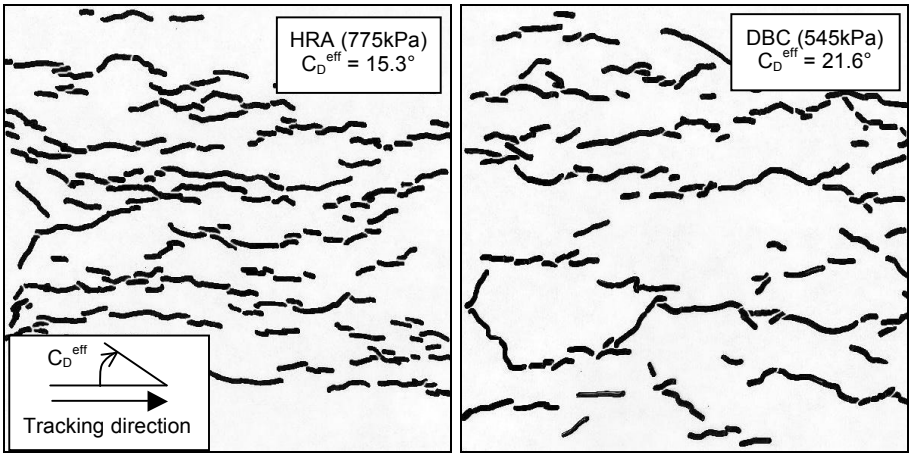

Figure 13. *Examples of final crack patterns.*

6.2. *Strain measurements*

Figure 14 describes the typical manner in which dynamic strain varied after different loading intervals. The strain results from the other pavement samples follow a similar trend and this behaviour is identical to that observed by Rowe [ROW 96].

By correlating these strain measurements against crack behaviour, it is observed that the initial strain level remains relatively constant until small cracks begin to

form on the bottom surface of the specimen. From this point onward, a continuing increase in the dynamic strain level implies that cracks are propagating underneath the gauge (Gauge 1 in Figure 14). A decrease, however, indicates that significant cracks are forming close to the gauge and that the material in this region is absorbing the strain, causing the gauge to detect reduced levels of strain (Gauge 2 in Figure 14). Due to the local strengthening effect caused by the epoxy, a larger percentage (±80%) of readings similar to Gauge 2 were observed.

The HRA mixture had greater fatigue wheeltracking strength than the DBC mix. The initial dynamic strain levels are plotted against the number of wheel loadings in Figure 15. On two of the DBC slabs debonding of the gauges occurred and data associated with these specimens are omitted.

Temperature does have an effect on the performance of bituminous mixtures [AIR 95]. The increased life exhibited by the HRA slabs is also thought to be a consequence of the lower temperature range to which they were exposed. The DBC specimens tested at the 80kg load also showed relative shorter lives compared to the other load settings. Significantly, these specimens were tested at a slightly higher temperature range than the DBC specimens that had been tested at both 100kg and 55kg.

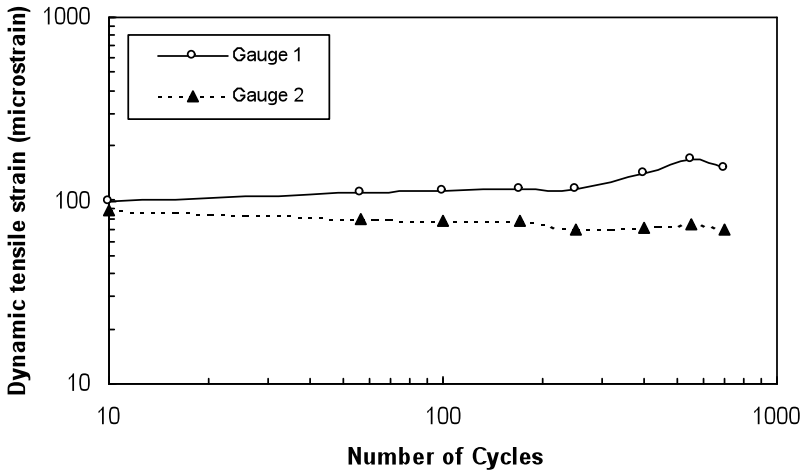

Figure 14. *Development of dynamic tensile strain under fatigue loading of DBC slab.*

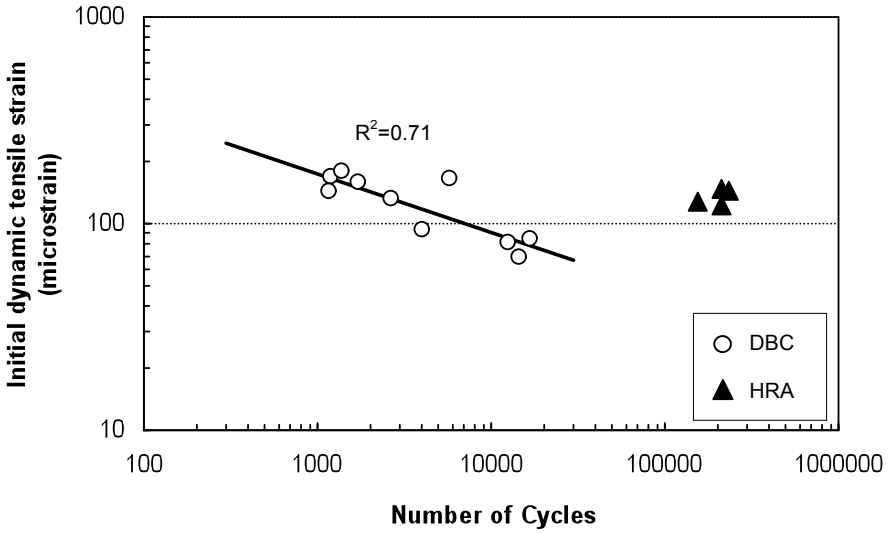

Figure 15. *Initial tensile strain versus number of load repetitions for wheeltracking slab specimens.*

7. Conclusions

For asphalt slabs that were simply supported on a weak elastomeric foundation and repeatedly tracked with a one directional dynamic wheel load, fatigue cracks were observed to initiate at the bottom surface of the slab and propagate upwards. Rather than one main crack appearing under the wheel track, small individual cracks opened along the bottom of the sample. These interconnected and combined to form a manner of network cracking. Once a full width crack had formed, this crack propagated through the depth of the slab. Typical behaviours that were observed during the development of crack area and crack length are illustrated in Figure 16. Measurements of crack length on the bottom face of the specimen can be used successfully to characterise the initial stage of crack formation (Stage I). The crack propagation phase (Stage II), on the other hand, is more successfully characterised by changes in the area of cracking.

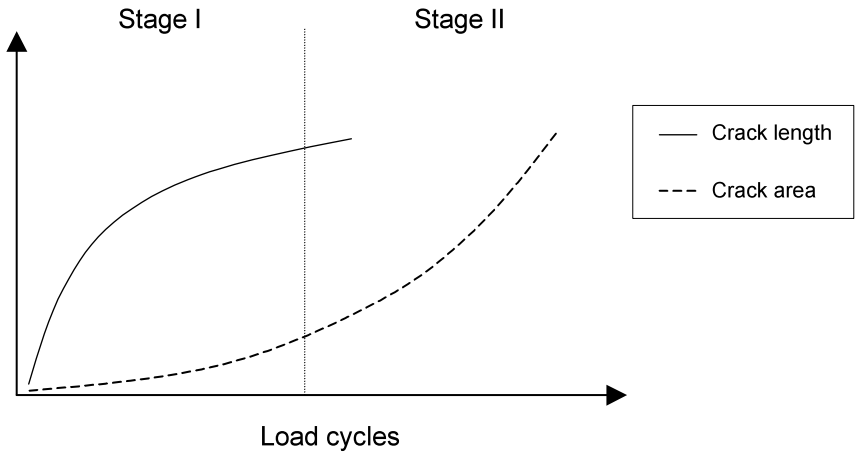

Figure 16. *Typical development of crack area and crack length during wheeltracking tests.*

The orientation of cracks remained relatively parallel to the direction of wheel travel throughout the fatigue life of a specimen. As the test load decreased, the direction of cracking veered slightly from the horizontal and the total length of cracks decreased. Although fewer cracks were observed on the HRA slabs, the orientation of these cracks was similar to those in the DBC slabs that had been tested under the same loading conditions.

8. Acknowledgements

The authors would like to express their gratitude to Dr Ian Jamieson and Mr Frank Clancy of the National Roads Authority, to Mr Michael Byrne of Roadstone Dublin Ltd. and to Enterprise Ireland (Applied Research Grants HE/1996/148 and HE/1998/288) for sponsoring this research. The support provided by Ms Amanda Gibney and Messrs Michael MacNicholas and Tom Webster of the Department of Civil Engineering at NUI,D is gratefully acknowledged.

9. References

[AIR 95] AIREY, G.D., 'Fatigue testing of asphalt mixtures using the laboratory third point loading fatigue testing system.' M. Eng. Thesis, University of Pretoria, South Africa, 1995.

[BS 93] BS 4987: PART 1, "Coated Macadams for roads and other paved areas." British Standards Institution, London, England, 1993.

[BS 92] BS 594: PART 1, "Hot Rolled Asphalt for roads and other paved areas." British Standards Institution, London, England, 1992.

[GIL 97] Gilchrist, M. D. & Hartman, A. M., 1997, *Performance Related Test Procedures for Bituminous Mixtures*. Boole Press, Dublin. 214pp.

[HAR 99] Hartman, A. M., Nolan, D. & Gilchrist, M. D., 1999, Experimental facility for simulating the initiation and propagation of fatigue damage in bituminous road paving materials. *Key Engineering Materials*, **167-168**, pp. 27-34.

[HAR 00] HARTMAN, A.M., 'An experimental investigation into the mechanical performance and structural integrity of bituminous pavement mixtures under the action of fatigue load conditions.' PhD Thesis, University College Dublin, Ireland, 2000.

[HAR 01a] Hartman, A. M., Gilchrist, M. D. & Walsh, G., 2001, Effect of mixture compaction on indirect tensile stiffness and fatigue. To appear in *ASCE Journal of Transportation Engineering.*

[HAR 01b] Hartman, A. M., Gilchrist, M. D., Owende, P., Ward, S. & Clancy, F., 2001, In-situ accelerated testing of bituminous mixtures. Submitted to *International Journal of Road Materials and Pavement Design*.

[LEE 93] LEE, J.; HUGO, F.; STOKOE, K.H., 'Using SASW for monitoring low-temperature asphalt degradation under the model mobile load simulator (MMLS).' Research Report 1934-2, Centre of Transportation Research, University of Texas at Austin, USA, 1993.

[OWE 01] Owende, P. M. O., Hartman, A. M., Ward, S. M., Gilchrist, M. D. & O'Mahony, M. J., 2001, Minimising distress on flexible pavements using variable tire pressure. *ASCE J. of Transportation Engineering*. **127** (3), pp. 1-9.

[ROW 96] ROWE, G.M., "Application of the dissipated energy concept to fatigue cracking in asphalt pavements." PhD. Thesis, University of Nottingham, England, 1996.

[SAI 00] SAID, S.F., "The VTI wheel tracking test." *Nordic Road and Transport Research*, No. 1-2000, 2000, p.19.

[TAB 89] TABATABAEE, N.; SEBAALY, P.; SCULLION, T., 'Instrumentation for flexible pavements.' FHWA Report RD-89-084, Washington USA, 1989.

[ULE 96] ULEAD SYSTEMS, 'Ulead PhotoImpact Version 3.0SE.' Ulead Systems International Inc., Taipei, Taiwan, 1996.

[ULL 87] ULLIDITZ, P.P., "Pavement analysis." Pub. Elsevier Science, Netherlands, 1987.

[UTH 96] UTHSCSA IMAGE TOOL, 'Image Tool Version 2.0.' University of Texas Heath Science Centre Department of Dental Diagnostic Science, San Antonio, Texas, USA, 1996.

[VAN 75] VAN DIJK, W., "Practical fatigue characterisation of bituminous mixtures." *Proceedings of the Association of Asphalt Paving Technologists*, vol. 44, 1975, p. 38-74.